Local orientational correlations and short time anisotropic motion in molecular liquids: Computer simulations of liquid CO 2

I. I. Fedchenia and J. Schröder

Citation: The Journal of Chemical Physics **106**, 7749 (1997); doi: 10.1063/1.473775
View online: http://dx.doi.org/10.1063/1.473775
View Table of Contents: http://scitation.aip.org/content/aip/journal/jcp/106/18?ver=pdfcov
Published by the AIP Publishing

Local orientational correlations and short time anisotropic motion in molecular liquids: Computer simulations of liquid CO_2

I. I. Fedchenia and J. Schröder
Max-Planck-Institut für Biophysikalische Chemie, Am Fassberg, D-37077 Göttingen, Germany

(Received 19 September 1996; accepted 7 February 1997)

Molecular dynamic (MD) simulations of liquid CO_2 at 250 MPa pressure and room temperature have been performed using a flexible model potential. A detailed analysis of the data reveal the full three-dimensional local structure of coordination shells that exhibit significant deviations from spherical symmetry with strong angular correlations among the molecules which form the inner coordination shell of the local liquid structure. Structures resembling T-shaped and offset-parallel CO_2 dimers similar to those found in molecular beam and low temperature experiments have been identified, the T-shaped dimer having higher probability to be formed than the offset-parallel configuration. Local motion on short time scale is found to be different along three principal directions of a local coordinate frame. © *1997 American Institute of Physics.*
[S0021-9606(97)51818-6]

I. INTRODUCTION

Most of structural data about the liquid state comes as radial pair correlation functions (or their Fourier transforms) from neutron scattering experiments. Unfortunately, some very interesting and important information is lost due to averaging over angle variables. This missing information can refer to both spatial arrangements of probability peaks and orientations of molecular pairs.

Although an indirect method to estimate the presence of orientational correlations in molecular liquids has been proposed a while ago,[1] it is not until recent works by Soper *et al.*[2–4] that the full three-dimensional reconstruction of pair distribution functions and some orientational properties have been performed explicitly for methanol in water, hydrogen halides, and pure water.

By definition, pair correlation functions account for dimer configurations of molecules in liquid. It is, therefore, interesting to compare configurations of molecular dimers well known from molecular beam experiments with configurations of the same species in condensed phase. Since its first discovery by Leckenby and Robbing in 1966,[5] the equilibrium conformation of the CO_2 dimer has been the subject of numerous theoretical and experimental investigations for nearly two decades. Several different conformations were proposed, but eventually discussion has been reduced to the distinction between two basic equilibrium structures, a T-shaped and an offset-parallel dimer. In particular, high resolution spectroscopic studies in low temperature matrices[6,7] and in molecular beams[8–11] suggest that at least under these conditions the offset-parallel dimer is the real stable species. Theoretical calculations[12] confirm that the energetically lowest conformations correspond to two equivalent offset-parallel, isomeric dimers, the T-shaped dimer being a transient structure between the two. The calculations show, however, that T-shaped and offset-parallel conformations are energetically very close to each other—according to Ref. 12 the energy difference is only 0.16 kJ/mol, i.e., negligibly small at room temperatures. One may, therefore, expect that the local dynamics in the room temperature liquid is characterized by persistent rapid transitions between the isomeric offset-parallel structures and controlled to a large extent by collective interactions in the liquid rather than by the potential energy surface describing the two body interaction.

The T-shaped and the offset parallel CO_2 dimers seem to be indistinguishable spectroscopically in condensed phase because the fine structure of optical spectra with the resolution[12] of $2-3\ \mathrm{cm}^{-1}$ is absent in this case. Therefore, experimentally the local orientational structure in the liquid can only be accessed by neutron scattering techniques. The first evidence on the existence of orientation correlations in liquid CO_2 was given by Adya and Wormald[13] using the abovementioned indirect method.[1] The difficulty in extracting details on how these correlations look like is in the fact that one has to make assumptions about their functional form before one can fit the experimental structure factor by a product of a calculated molecular centre structure factors and a corresponding orientational part.[1] It is, therefore, of prime importance to access information about orientational correlations directly. For this reason, we performed a 3D analysis of MD trajectories calculated for liquid CO_2 at a temperature of 300 K and 250 MPa pressure. These results show that the local shell structure exhibits significant anisotropy and pronounced effects of molecular flexibility. Here we wish to investigate to what extent this anisotropic structure correlates with distinct local orientational pattern of liquid CO_2. The information that we derive from our analysis can be compared directly with results that one extracts form neutron scattering experiments using spherical harmonic reconstruction methods.[2–4]

We found that the pair distribution functions reported in this paper possess strong angular dependence at short distances. This fact must reflect on short time dynamics of individual molecule. One can expect pronounce anisotropy of averaged motion for times correspondent to the passage across the first probability maximum. We demonstrated this

by calculating mean square distances in three perpendicular directions in the local frame.

II. MODEL POTENTIAL AND COMPUTATIONAL DETAILS

Among the various choices of intermolecular pair potentials that have been proposed for the CO_2–CO_2 interaction (see Ref. 12 for an overview) we have chosen the one that gives the best agreement with experimental data from neutron scattering[13–15] in liquid CO_2,

$$U_{ij}=\exp\left(-\frac{R_{ij}-\sigma_i-\sigma_j}{\rho_i-\rho_j}\right)+\frac{q_iq_j}{R_{ij}}-\frac{C_{ij}^{(6)}}{R_{ij}^6}F_{ij}(R_{ij}).$$

with

$$F_{ij}(R_{ij})=\exp\left\{-\left[\exp\left(-\frac{1.28\cdot R_{ij}^0}{R_{ij}-1}\right)\right]^2\right\}$$

$$\text{if } \frac{1.28\cdot R_{ij}^0}{R_{ij}-1}>1$$

$$=1 \quad \text{otherwise,}$$

where $\{i,j\}$ stand for {C,O}, R_{ij} denotes the interatomic distance, and q_i is the partial charge on atom i. The parameter values[14,15] are given in atomic units,

$$R_{ij}^0=2.65;\ \ C_{ij}^{(6)}=21.4;\ \ \sigma_C=0.77;\ \ \sigma_C=1.23;$$

$$\rho_C=0.25;\ \ \rho_O=0.24;\ \ q_C=1.040;\ \ q_O=-0.52.$$

We modified the potential to model the flexibility of the CO_2 molecule by including an appropriate set of parameters for the stretching and the bending vibrational modes,[16,17]

$$U_{\text{intra}}=\frac{k_b}{2}(b_1^2+b_2^2)+k_{bb}b_1b_2+\frac{4\cdot k_{\text{bend}}}{1-\cos\,\theta},$$

where b_1 and b_2 are the two C–O bond lengths and θ is the OCO bond angle. The values of the force constants are in dyn/cm, $k_b=1.55\cdot 10^6$, $k_{bb}=1.3\cdot 10^5$, $k_{\text{bend}}/b_0^2=5.7\cdot 10^4$, with the gas phase bond length $b_0=1.161\cdot 10^{-8}$ cm. This original parameter set fails to reproduce most of thermodynamical quantities and has to be corrected for each particular density. At the lower density, 0.743 kg/m^3 slightly above critical point, we used a partial charge $q_C=0.64$ and had to increase $C_{ij}^{(6)}$ by a factor of 2.5 to obtain the correct experimental pressure. We used then this corrected value for $C_{ij}^{(6)}$ at higher density 1.2 kg/m^3 and increased q_C up to 0.815 to obtain the correct experimental pressure of 250 MPa. In our simulation the value $q_C=1.040$ given in Refs. 14 and 15 results in an incorrect pressure of 350 MPa at 300 K. We would like to pay attention to the necessity of changing partial charges and $C_{ij}^{(6)}$ at the same time. One could, in principle, get the correct experimental pressure manipulating partial charges alone but the other thermodynamical quantities (diffusion coefficient, viscosity, dielectric constant, etc.) are out of order in that case. Varying partial charges of the potential together with the dispersion parameter and slightly changing parameters of short range repulsive forces we have been able to reproduce experimental values for pressure, diffusion coefficient, and viscosity of CO_2 at room temperature for densities between 0.743 kg/m^3 and 1.2 kg/m^3 to within experimental uncertainty. The value for the static dielectric constant is within 15%–25% of experimental value, being systematically lower throughout the density range without any additional adjustment of the potential parameters.

We would like to point out significant differences in the conclusions drawn from neutron scattering in liquid[13] CO_2 and high-resolution infrared spectroscopy of jet-cooled[18] $(CO_2)_2$ and $(CO_2)_3$ concerning the question which specific model pair potential best fits the experimental data. In the latter study, spectral evidence rules out the *T*-shape conformation, and, therefore, according to Ref. 18 the model pair potential developed in Refs. 14 and 15 should not be used because it gives an energy minimum at the *T*-shape structure (although only by 0.03 kJ/mol lower than for the offset-parallel conformation). However, the fact that it best fits the neutron scattering data for liquids has led us to choose it as a starting point for our MD simulations of CO_2 in the compressed liquid phase. As there are no high resolution spectroscopic data for liquid CO_2, the only option left for adjustment of the intermolecular potential parameters is to fit them to thermodynamical and transport data measured under the corresponding physical conditions.

These considerations about the details of the molecular pair interaction are in line with the results of Ref. 19 where it has been shown that the presence or absence of the minimum at the T-shape conformation is determined by a delicate balance between the electrostatic interaction (which favors T-shape form) on the one hand, and dispersion and repulsive forces on the other hand which destabilize this conformation. The fact that there exists a corresponding combination of values for the partial charges and the dispersion coefficients which yields the best fit of the experimental data, make us believe that our potential parameter set used for the simulation of compressed liquid CO_2 represents the best choice for our purposes. A very recent attempt[20] to use an *ab initio* pair potential, resulted from calculations with the largest ever used for the CO_2 basis set, in MD simulations of liquid phase confirms once again what has become a common belief in the MD community for some time; a pair potential which perfectly fit spectroscopic experimental data in diluted gases and molecular beams fails miserably when applied to liquid phase without any special adjustment. The possible reasons seem to be the absence of polarizability in the model and neglect of multibody effects; the latter fact manifests itself in the dependence of our parameter set on thermodynamic state.

A cubic box with 512 carefully equilibrated molecules has been used for calculations of spatial distribution functions. Each molecule in the box has been supplied with the local coordinate frame as shown in Fig. 1. Neutron sources with $Q\geqslant 10$ Å^{-1} provide essentially momentary snapshots of the liquid that requires us to put the origin of the local coordinate frame on one of the nuclei. A slightly instant bend allows us to determine the orientation of the local coordinate frame uniquely that would be impossible for a completely stiff model. We, then, calculated $\cos^2(zz)$ and $\cos^2(zn)$ between the *z* molecular axes of each pair and *z* molecular axis of one molecule and radius vector *n* to the C atom of the other. In this way we accumulate the statistics of the mutual

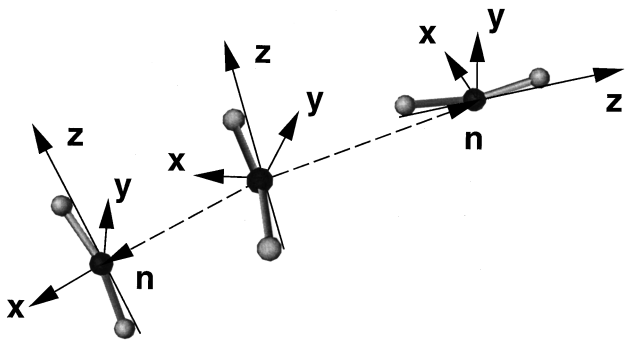

FIG. 1. Local molecular frames used for the calculation of orientational correlation functions $\cos^2(zz)$ and $\cos^2(zn)$ in liquid CO_2. The right pair depicts the T-shape, the left one the offset-parallel dimer.

orientational angles, each molecule being used as a reference one in turn. Statistics of a single snapshot is not enough to observe the second and the third spatial shells. The system therefore has been propagated in time for 40 ps using a multistage velocity Verlet algorithm (a time step for intramolecular vibrations is 10 times shorter than a time step for intermolecular motion which is equal to 1 fs) before the next snapshot has been taken. Each spatial distribution presented here is the result of 100 of such snapshots.

III. SPATIAL PAIR DISTRIBUTION FUNCTIONS

A spatial distribution function is a complex four-dimensional object. There are several possibilities to visualize it. Here we use an approach similar to that one used in Refs. 21 and 22 to visualize spatial structures found in water and methanol.

Isosurfaces of the C–C spatial distribution functions are shown in Figs. 2 and 3 at decreasing levels of probability. We count the probability level from the maximum of the pair distribution function.

At the highest level of probability, Fig. 1(a), we observe structured rings perpendicular to the molecular O–C–O axis, which shows an asymmetry caused by flexibility of the model. The probability is higher towards the convex side of the CO_2 molecule than towards the concave side. If one decreases the probability level by 10%, Fig. 2(b), a complete ring around the reference molecule builds up and its asymmetry becomes less pronounced. In addition, the outer ring structures perpendicular to the O–C–O-axis have developed into caps which face the terminal O-atoms of the reference CO_2 molecule.

Decreasing the probability level by another 25% reveals the existence of a complete solvation shell with strong deviation from spherical symmetry as can be seen in Fig. 2(c). Moreover, the second outer shell structure begins to develop. In Fig. 2(d) we have decreased the level by an additional 5%, and apart from the completing of the two outer spherical shells, we also find a new outermost shell of perfect spherical symmetry which we call ''the bulk shell'' because it corresponds to the isotropic distribution of remote trial molecules. Lowering the level further by another 10% in Fig. 3(a) we observe that the first shell gradually disappears leaving in its place the innermost shell with strong asymmetry that we call

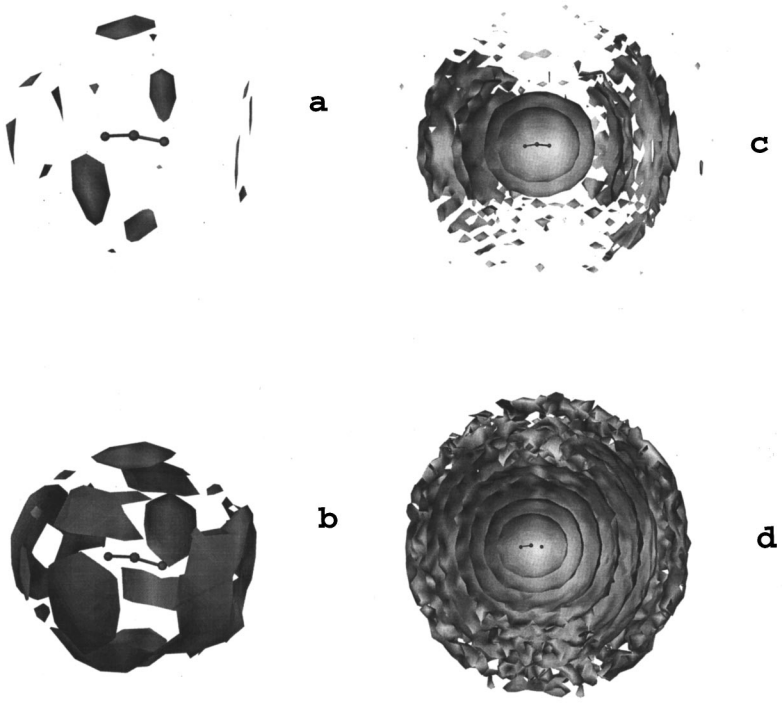

FIG. 2. Isosurface of the spatial C–C pair distribution function at the level of (a) 0.84 of the first maximum; (b) 0.73; (c) 0.5, cross section in the O–C–O-plane, and (d) 0.45, cross section in the O–C–O-plane, showing the collision shell, three peaks and the bulk shell.

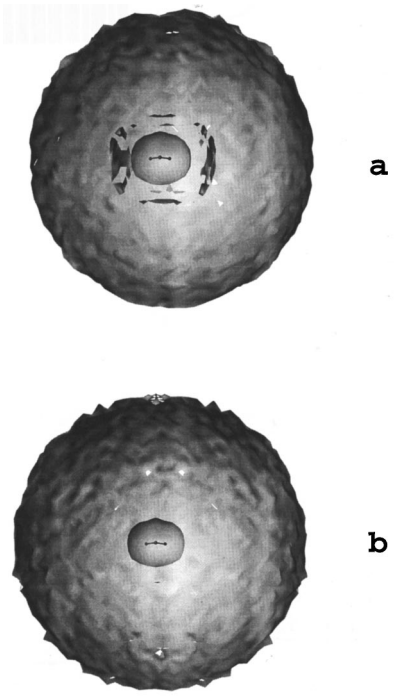

FIG. 3. Cross section in the O–C–O-plane of isosurfaces of the spatial C–C distribution function at the levels of (a) 0.32 of the first maximum, showing the collision shell, the remainder of the first shell and the bulk shell; and (b) 0.27, showing low probability events i.e. the most energetic collisions with only the collision shell and the bulk shell appearing.

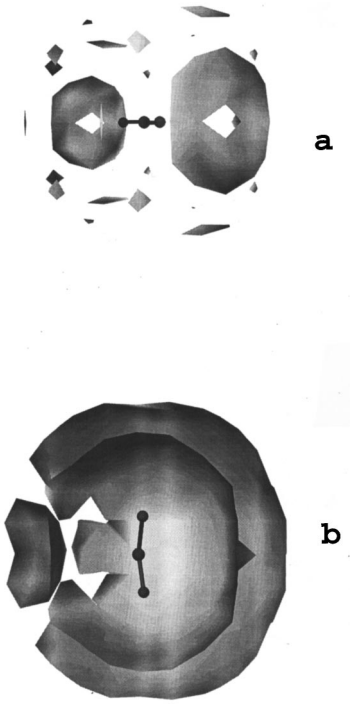

FIG. 4. Isosurfaces of the spatial C–O pair distribution function at the level of probability (a) 0.94 of the first peak (cross section perpendicular to the molecular axis); and (b) 0.85 (cross section in the O–C–O-plane) showing the effect of bent geometry.

''the collision shell,'' because it corresponds to the distance of closest approach of two CO_2 molecules. And finally decreasing the probability level to 1/8 of the maximum value in Fig. 3(b) leaves only the collision and the bulk shell intact. The collision shell now represents molecules that collide with the highest kinetic energy. In following the build-up and the destruction of solvent shells through Figs. 2 and 3 it is interesting to note the high degree of anisotropy in the different stages. We demonstrate later that this local anisotropy of the liquid structure of highly compressed CO_2 has consequences for the detailed dynamics and spatial dependence of collisional energy transfer.

In Figs. 4 and 5 we show corresponding isosurfaces of the CO spatial pair distribution function. Comparing Figs. 2 and 4 one realizes that the maxima of the CC and the CO structure are complementary. Figure 4(b) demonstrates the influence of the molecular flexibility on the asymmetry of the first and second shells. A lower level of probability was chosen in Fig. 5 revealing the shell structure (only a slice of 0.2 nm thickness is shown for clarity) and the asymmetry of the collision shell.

IV. SPATIAL PATTERNS OF ORIENTED PAIRS

We would like to find out whether any special orientational configurations exist in liquid CO_2 and if so what are their mutual spatial positions. Of course, one cannot expect to find ''pure'' T-shaped or offset parallel conformations in the liquid because they will be obscured by persistent strong thermal fluctuations. However, values of $\cos^2(zz)$ greater than 0.5 or closer to zero in certain regions of the spatial liquid structure correspond to configurations with a tendency towards the offset-parallel or T-shaped conformation of pairs of CO_2 molecules, respectively.

In Fig. 6, we show isosurfaces for two low values of $\cos^2(zz)$ corresponding to a predominantly T-shaped average orientation. They are overlapped with isosurfaces of the spatial pair correlation function corresponding to the position of the first peak [Fig. 2(a)] and to the appearance of a shell structure [Fig. 2(c)]. It is evident that the ring around the C-atom of the reference molecule is dominated by T-shaped orientations. The inner isosurface of $\cos^2(zz)$ reflects the low probability collision shell (Fig. 3) which also shows a preference of T-shaped geometry during collisions. The complementary picture for offset-parallel average orientation is shown in Figs. 7(a) and 7(b) where the isosurface corresponds to an average level of $\cos^2(zz)$ equal to 0.6 (a) and to 0.39 (b). The regions of the most predominant offset-parallel type orientation corresponds to those with rather low probability level of the spatial pair distribution function that is roughly a by factor of 5 lower than for the regions where one observes a predominance of T-shape orientations. An interesting feature of Fig. 7(b) is that the part of the first shell of the CC probability distribution function possesses offset-parallel orientation [outer rings in Fig. 3 (b)].

An independent statistical test to verify that the isosurfaces of $\cos^2(zz)$ actually correspond to the spatial distribution of the average relative pair orientation shown in Figs. 6 and 7 is to compare them with isosurfaces of $\cos^2(zn)$, the average angle between the radius vector pointing from the

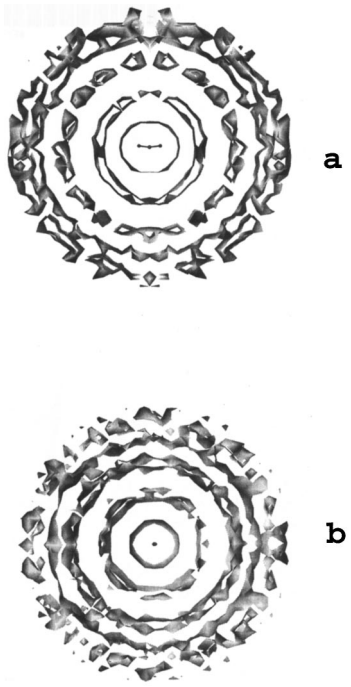

FIG. 5. Slices of 0.2 nm thickness cut out of isosurfaces of the C–O pair distribution function at the level of probability 0.68 of the first peak (a) in the C–O–O-plane and (b) perpendicular to the molecular axis.

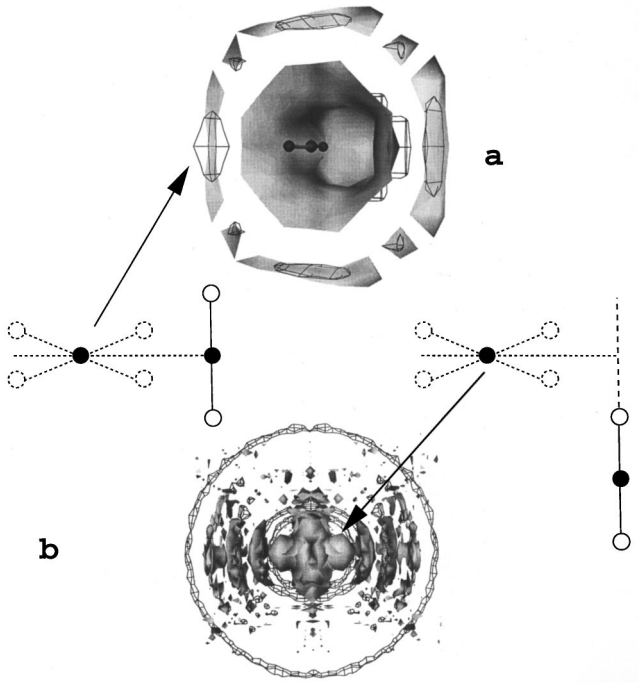

FIG. 6. Overlap of the $\cos^2(zz)$ (shaded) and C–C spatial pair distribution function (wire) isosurfaces at average values and probability levels, respectively, of (a) 0.22 and 0.81; and (b) 0.31 and 0.4. The arrows indicate the regions of the spatial pair distribution function corresponding to predominantly T-shaped dimers. The inner surfaces in (a and b) correspond to the low probability collision shell, Fig. 3. Parts of the shells in (b) exhibit a significant degree of orientation.

reference C-atom to that of the trial molecule and molecular axis of the trial molecule. The result is shown in Figs. 8 and 9; regions of predominantly T-shaped orientations having a low value of $\cos^2(zz)$ and a high value of $\cos^2(zn)$ and those of higher probability of parallel orientations with high $\cos^2(zz)$ and a low $\cos^2(zn)$ show a significant overlap indeed. We also note that all spatial distributions of orientational correlations shown here also reflect the effects of molecular flexibility in the sense that there is no rotational symmetry around the molecular axis.

V. ANISOTROPY OF LOCAL MOTION ON SHORT TIME SCALE

Figures 2(a)–2(d) reveal a strong anisotropy of probability density on the spatial scale of 1–1.5 nm. One can expect therefore that local dynamics on the short time scale also reflect this anisotropy in some way. Figure 10 demonstrates the difference in diffusion of a CO_2 molecule in three different directions $\{x, y,$ and $z\}$ determined by the local frame for each individual molecule (Fig. 1). For both low (7.5 MPa) and high (250 MPa) pressure one can distinguish three different time domains with qualitatively distinct behavior; very short (about 100 fs) initial period when the time behavior of the target particle is purely dynamical, $\langle (x-x(0))^2 \rangle$, is proportional to t^2; the intermediate regime of nonclassical diffusion, $\langle (x-x(0))^2 \rangle$, is proportional to t^α and final classical diffusion stage where $\langle (x-x(0))^2 \rangle = 2Dt$, where D is a diffusion coefficient.

Several studies in the past[23–25] attempted to define geometrical properties of a trajectory of a single molecule in condensed phase. These attempts were evidently inspired by Mandelbrot's monograph[26] where it has been stated that fractal dimension of the trajectory of a single species in an N-particle system d_F is 2 for large N. That implies that the trajectory can essentially be modeled by classical Brownian motion. The works[23–25] have shown, however, that the situation is more complicated that it has been originally suggested.[26] It has been found for several models that the trajectory of a single molecule possesses variable fractal dimensionality ranging from 1 for very short scale to 2 for very long scale dependent upon the size of the scale used to measure the trajectory length. Following the argumentation of Ref. 24 it is easy to show that the coefficient α and the fractal dimension of the trajectory d_F are connected by the simple formula $\alpha = 2/d_F$ which means that considerations[23–25] on dependency of d_F on a spatial scale can be transferred to the time domain. In other words, α depends on the time interval that is used to measure the increment of the particle position $\Delta \mathbf{r}$ $\alpha = 2 (d_F = 1)$ suggests that for that time scale the motion is ''dynamiclike'' and for $\alpha = 1 (d_F = 2)$ it is classically diffusive. The underlying physical reason for that scale dependence can be understood from comparison of the time scales with different behavior for $(\Delta \mathbf{r})^2$ and those for velocity autocorrelation function.[27] One can see that the first initial period of about 200 fs with $\alpha = 2 (d_F = 1)$ coincides approximately with the time of the first zero crossing of velocity autocorrelation function.[17] This time it is attributed to the loss of memory due to reflections from the molecular cage.[27] From Fig. 10(a) one can observe that for the CO_2 molecule

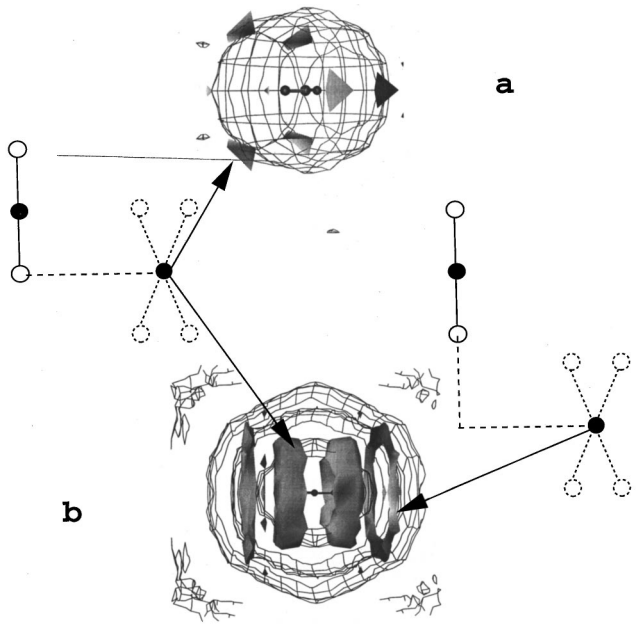

FIG. 7. Overlap of the $\cos^2(zz)$ (shaded) and C–C spatial pair distribution function (wire) isosurfaces at average values and probability levels, respectively, of (a) 0.6 and 0.21; and (b) 0.39 and 0.48. The arrows indicate the regions of the spatial pair distribution function corresponding to predominantly offset-parallel dimers.

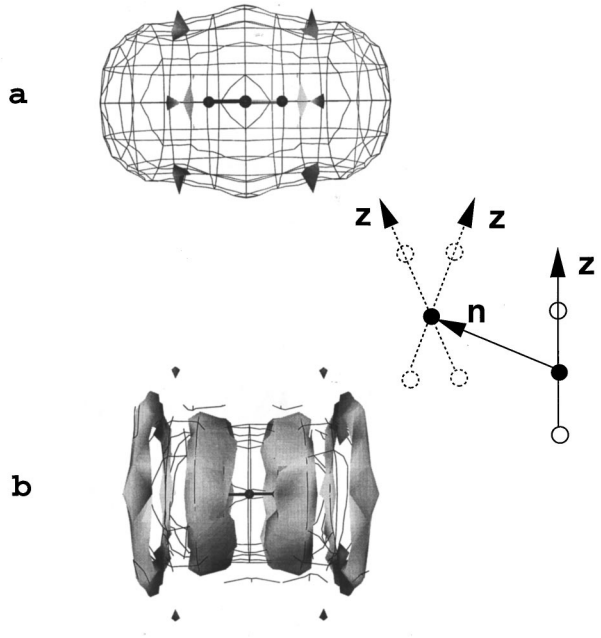

FIG. 9. Overlap of the $\cos^2(zz)$ (shaded) and $\cos^2(zn)$ (wire) isosurfaces at average values, respectively, of (a) 0.6 and 0.12; and (b) 0.39 and 0.21. The conformation shown schematically corresponds to the two inner rings.

moving in an anisotropic environment this initial ''dynamic'' period is different for the motions along and perpendicular to the molecular axis, being longer (especially for the low density) in the z direction due to the low probability for the target molecule to meet the first neighbor as it is clear from Fig. 2. An interesting thing is that a time scale exists where $\langle (x-x(0))^2 \rangle$ is proportional to t^{α} with $\alpha \neq$ (1 or 2) that is

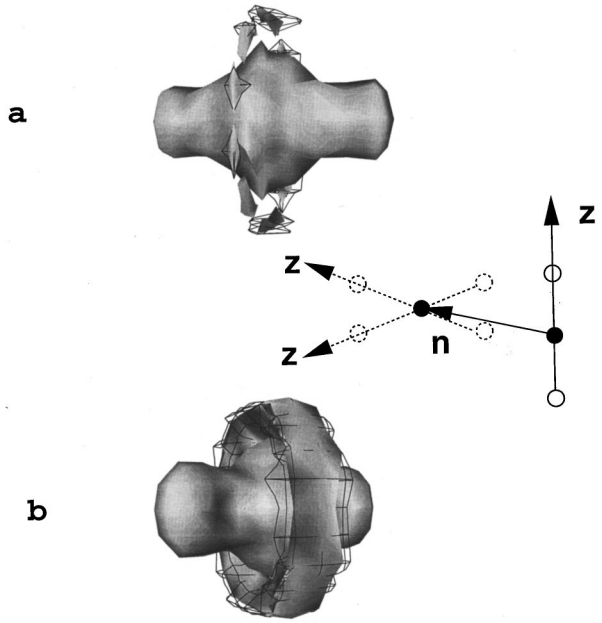

FIG. 8. Overlap of the $\cos^2(zz)$ (shaded) and $\cos^2(zn)$ (wire) isosurfaces at average values, respectively, of (a) 0.22 and 0.54; and (b) 0.25 and 0.5. The conformation shown schematically corresponds to the outer ring.

density dependent. As it can be seen from Fig. 10 this scaling range lasts from 200 fs to 1 ps and overlaps approximately with the negative part of the CO_2 velocity autocorrelation function.[17] That suggests that the physical reason for this anomalous behavior is the molecular motion in random potential of the cage which results in the broad distribution of vibrational frequencies for that motion. In the ultimate case of the low density, Fig. 10(a) the motion in z direction has $\alpha = 2$ and, therefore, is ''dynamiclike'' due to the very small amount of colliding centers in the z direction of the local frame of every molecule. This period of anomalous motion $[a \neq$ (1 or 2)] is substantially shorter than that one found recently[28] for diffusion of water in the vicinity of the large macromolecule. It has been explained by the fractal dimension of the protein surface.

In sufficiently long time the difference of diffusion in three different directions vanishes similarly to the disappearance of spatial anisotropy with distance shown in Fig. 1(d). On the short time scale, however, the difference between motion in the three different directions is very well pronounced. A similar effect has been found earlier[29] for self-diffusion of CS_2 and OCS in argon.[30,31] For the low pressure diffusion in the direction of the molecular axis is much faster than in direction of the other two. In addition to that, for the high pressure one can observe the difference between motion perpendicular to the plane of molecular bending {y direction} and in the bending plane perpendicular to the molecular axis z {x direction}. This can be easily understood from Figs. 2(a) and 2(c), where the probability to find another CO_2 molecule for collision is substantially larger in the direction perpendicular to the molecular axis z.

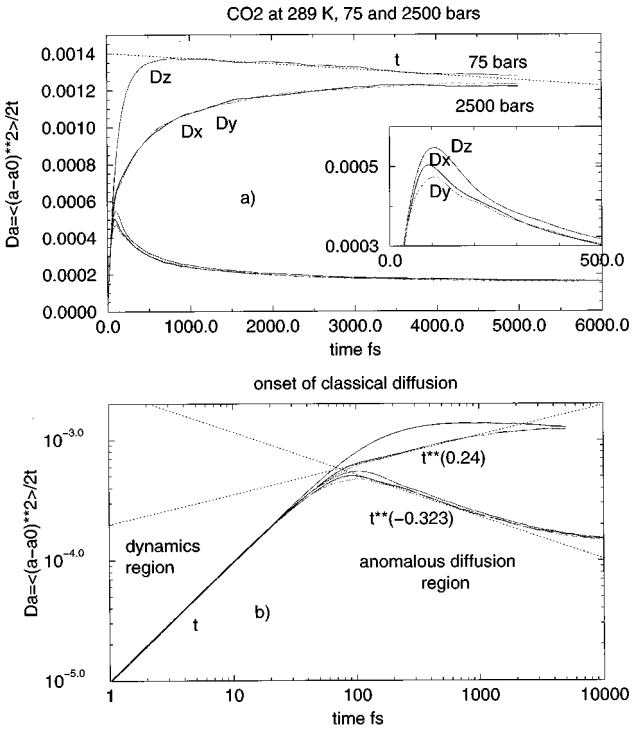

FIG. 10. Anisotropy of self-diffusion motion in three perpendicular directions defined in the local frame, Fig. 1, for two different pressures. (a) Linear scale and (b) log–log scale showing three stages of diffusion motion. Remarkable is a rather long period of ''dynamic'' like motion in the z direction for the low density (a).

VI. CONCLUSION

We presented a detailed 3D-structural analysis of highly compressed liquid CO_2 at 250 MPa and room temperature based on spatial pair correlation function derived from MD simulation using a flexible model potential. The potential was adjusted to reproduce the pressure–density isotherm at 298 K. The simulations reveal substantial local anisotropy of this nonpolar liquid on a scale of 1–1.5 nm. We also observe a notable influence of the molecular flexibility that manifests itself in the broken symmetry of pair distribution functions, orientational properties, and diffusion in bending plane. Similar to the recent theoretical work[32] and experimental results supported by molecular dynamics simulations[33,34] we found that T-shape like orientation prevails in the liquid. However, our calculations suggest that orientations corresponding to offset-parallel can be found as well although with lower probability than the T-shape ones. We demonstrate also that this local spatial anisotropy reflected on the local dynamics on short time scale that results in the difference of local diffusion rate in three perpendicular directions.

ACKNOWLEDGMENTS

The authors would like to thank Professor Dr. J. Troe for constant encouragement and generous support and Dr. P. Vöhringer and Dr. D. Schwarzer for many helpful discussions.

[1] P. A. Egelstaff, D. I. Page, and L. G. Powles, Mol. Phys. **20**, 881 (1971).
[2] A. K. Soper and J. L. Finney, Phys. Rev. Lett. **71**, 4346 (1996).
[3] A. K. Soper, C. Andreani, and N. Nardone, Phys. Rev. E. **47**, 2598 (1993).
[4] A. K. Soper, J. Chem. Phys. **101**, 6888 (1994).
[5] R. E. Leckeenby and E. J. Robbing, Proc. R. Soc. London **291A**, 389 (1966).
[6] R. Guasti, V. Schettino, and N. Bigot, Chem. Phys. **34**, 39 (1978).
[7] A. E. Barton, A. Chablo, and B. J. Howard, Chem. Phys. Lett. **60**, 414 (1979).
[8] K. W. Jucks, Z. S. Huang, D. Dayton, R. E. Miller, and W. J. Lafferty, J. Chem. Phys. **86**, 4341 (1987).
[9] M. A. Walch, T. E. England, T. R. Dyke, and B. J. Howard, Chem. Phys. Lett. **142**, 265 (1988).
[10] K. W. Jucks, Z. S. Huang, R. E. Miller, G. T. Fraser, A. S. Pine, and W. J. Lafferty, J. Chem. Phys. **88**, 2185 (1988).
[11] A. S. Pine and G. T. Fraser, J. Chem. Phys. **89**, 100 (1988).
[12] L. M. Nxumalo and T. A. Ford, J. Mol. Struct. **327**, 145, 153 (1994).
[13] A. K. Adya and Ch. J. Wormald, Mol. Phys. **74**, 735 (1991).
[14] H. J. Böhm, R. Ahlrichs, P. Scharf, and H. Schiffer, J. Chem. Phys. **81**, 1389 (1984).
[15] H. J. Böhm, C. Meissner, and R. Ahlrichs, Mol. Phys. **53**, 651 (1984).
[16] G. Herzberg, *Molecular Spectra and Molecular Structure II. Infrared and Raman Spectra of Polyatomic Molecules* (Van Nostrand Reinhold, New York, 1945).
[17] S.-B. Zhu and G. W. Robinson, Comp. Phys. Commun **52**, 317 (1989).
[18] M. J. Weida, J. M. Sperhac, and D. J. Nesbitt, J. Chem. Phys. **103**, 7685 (1995).
[19] J. S. Muenter, J. Chem. Phys. **94**, 2781 (1991).
[20] M. Welker, G. Steinebrunner, J. Solca, and H. Huber, Chem. Phys. **213**, 253 (1996).
[21] I. M. Svischev and P. G. Kusalik, J. Chem. Phys. **99**, 3049 (1993).
[22] I. M. Svischev and P. G. Kusalik, J. Chem. Phys. **100**, 5165 (1994).
[23] J. J. Erpenbeck and E. G. D. Cohen, J. Stat. Phys. **43**, 343 (1985).
[24] Ch. L. Brooks III, Phys. Rev. A **35**, 5178 (1987).
[25] J. G. Powles and R. F. Fowler, Mol. Phys. **62**, 1085 (1987).
[26] B. B. Mandelbrot, *The Fractal Geometry of Nature* (Freeman, San Francisco, 1982).
[27] R. M. Lynden-Bell, D. J. Hutchinson, and M. J. Doyle, Mol. Phys. **58**, 307 (1986).
[28] A. R. Bizzarri and S. Cannistraro, Phys. Rev. E **53**, R3040 (1996).
[29] D. J. Tildesley and P. A. Madden, Mol. Phys. **48**, 129 (1983).
[30] J. Samios, D. Dellis, and H. Stassen, Chem. Phys. **178**, 83 (1993).
[31] D. Dellis and J. Samios, Chem. Phys. **192**, 281 (1995).
[32] A. F. Teerzis and E. T. Samulski, Chem. Phys. Lett. **251**, 157 (1996).
[33] R. Ishli, S. Okazaki, I. Okada, M. Furusaka, N. Watanabe, M. Misawa, and T. Fukunaga, J. Chem. Phys. **105**, 7011 (1996).
[34] S. Chiappini, M. Nardone, F. P. Ricci, and M. C. Bellissent-Funel, Mol. Phys. **89**, 975 (1996).